AIAA JOURNAL
Vol. 44, No. 1, January 2006

Active and Passive Control of Supersonic Impinging Jets

Huadong Lou,* Farrukh S. Alvi,† and Chiang Shih‡
Florida A&M University–Florida State University, Tallahassee, Florida 32310

The behavior of supersonic impinging jets is dominated by a feedback loop due to the coupling between the fluid and acoustic fields. This leads to many adverse effects when such flows occur in short takeoff and vertical landing aircraft, such as a significant increase in the noise level, very high unsteady loads on the nearby structures, and an appreciable loss in lifting during hover. In earlier studies, it was demonstrated that by using supersonic microjets one could disrupt the feedback loop that leads to substantial reductions in the aforementioned adverse effects. However, the effectiveness of control was found to be strongly dependent on the ground plane distances and the jet-operating conditions. The effect of various microjet control parameters are investigated in some detail to identify their influence on control efficiency and additional insight is provided on the physical mechanism behind this control method. Parameters studied include microjet angle, microjet pressure, and the use of microtabs instead of microjets. These results indicate that by choosing appropriate control parameters it should be possible to devise a control strategy that produces optimal control for the entire operating range of conditions of the supersonic impinging jet. Moreover, the experimental results provide convincing evidence of the generation of significant streamwise vorticity by the activation microjets. It is postulated that the generation of streamwise vorticity and its evolution in the jet flow might be one of the main physical phenomena responsible for the reduction of flow unsteadiness in impinging jets.

I. Introduction

THE flowfield generated by the impingement of high-speed lift jets on a surface usually results in a very unsteady flowfield. When such jets are used to generate direct lift in short takeoff and vertical landing (STOVL) aircraft during hover, this flow can lead to a host of adverse effects that can diminish aircraft performance. Significant among these are the substantially higher ambient noise levels in the jet vicinity and very high unsteady pressure loads on the ground plane and nearby structures. Frequently, the noise and the unsteady pressure spectra are dominated by high-amplitude discrete tones, which can further aggravate the sonic fatigue problem. These problems are more significant for supersonic impinging jets, the operating regime of the STOVL version of the Joint Strike Fighter.

A host of studies on the aeroacoustics of impinging jets by Powell,[1] Neuwerth,[2] Tam and Ahuja,[3] and more recently Krothapalli et al.[4] have clearly established that the self-sustained, highly unsteady behavior of the jet and the resulting impinging tones are governed by a feedback mechanism. The instability waves in the jet that originate at the nozzle exit grow as they propagate downstream toward the impingement surface, and the acoustic waves that are produced on impingement travel upstream and excite the nascent shear layer near the nozzle exit. For further details of the feedback loop, the reader is directed to Refs. 1–4. The acoustic properties of a single supersonic impinging jet flowfield have been investigated by a number of researchers[1–4] and continue to be the focus of current research. The emphasis is now increasingly on identifying control strategies to reduce the aforementioned problems associated with this flow because it is evident that such supersonic impinging jets need to be controlled to minimize their adverse influence on aircraft performance.

Powell[5] advocated viewing the resonant screech loop as a limit cycle. Four factors were considered in this limit-cycle approach: 1) the instability wave growth, 2) the shock–instability wave interaction, 3) feedback efficiency, and 4) stream disturbance creation efficiency. The last factor is commonly referred to as receptivity, and the second factor, in supersonic impinging jet, is the instability wave–impingement surface interaction.

Based on these ideas, a variety of control approaches have been proposed. One class of control methods attempts to manipulate the shear layer near the nozzle lip to make it less receptive to the acoustic disturbances, thus suppressing the formation of the feedback loop. This concept generally involves a modification of the nozzle geometry and the exit flow conditions using tabs[6] or nonaxisymmetric nozzle shapes.[7] Tabs have been shown to eliminate or reduce screech tones, where, for some cases, the mixing and shock-associated noise is reduced at lower frequencies but increases at higher frequencies. Using a nozzle with a design Mach number of 1.36, Samimy et al.[6] demonstrated that by using four tabs, the overall sound pressure level (OASPL) was reduced by about 6.5 dB when the jet was operated at an underexpanded mode. However, the reduction in noise was accompanied by a thrust penalty.

Another method for suppressing the feedback loop is to intercept the upstream and/or downstream propagating acoustic waves so that they cannot complete the feedback loop. Some attempts based on this idea have also been made. For instance, Karamcheti et al.[8] successfully suppressed edge tones in low-speed flows, which is governed by a similar feedback mechanism, by placing two plates normal to the jet centerline. Motivated by their work, Elavarasan et al.[9] used a similar technique to attenuate the feedback loop in a supersonic impinging jet by introducing a control plate just outside the nozzle exit. This passive control method resulted in a reduction in the near-field OASPL by about 6–7 dB.

Similarly, Sheplak and Spina[10] used a high-speed coflow to shield the main jet from the near-field acoustic disturbances. For a suitable ratio of the main jet and coflow exit velocity, they measured a reduction of 10–15 dB in the near-field broadband noise level in addition to the suppression of impinging tones. However, the mass flow needed for the coflow to achieve this makes this approach impractical. Shih et al.[11] successfully used counterflow near the nozzle exit to suppress screech tones of nonideally expanded jets. They were also able to obtain modest reductions in OASPL, approximately 3–4 dB, while enhancing the mixing of the primary jet.

Presented as Paper 2001-3027 at the AIAA 31st Fluid Dynamics Conference, Anaheim, CA, 11–14 June 2001; received 10 September 2004; revision received 12 July 2005; accepted for publication 18 August 2005.

*Graduate Research Assistant, Department of Mechanical Engineering, 2525 Pottsdamer Street. Student Member AIAA.

†Associate Professor, Department of Mechanical Engineering, 2525 Pottsdamer Street. Senior Member AIAA.

‡Professor and Chairman, Department of Mechanical Engineering, 2525 Pottsdamer Street. Associate Fellow AIAA.

Although a few of these techniques have produced some benefits, any significant performance gains were confined to a limited range of operating conditions, especially for impinging jets. This is because a relatively small change in the nozzle-to-ground separation (h/d) can lead to a significant change in the magnitude and frequency of the tones that are responsible for the undesired flow unsteadiness.[12] Therefore, an efficient control technique aimed at suppressing the feedback loop must adapt to the shift in frequencies/wavelengths of the modes that lock on to the feedback loop.

Recently, a new technique, which uses a high-energy fluid stream to modify the jet shear layer and thus disrupt the azimuthally coherent interaction between the flow instabilities and the acoustic field, was first developed and explored by Alvi et al.[13] and Shih et al.[14] The proposed control system has the advantage that, depending on the operating flow conditions, optimal flow control can in principle be achieved by activating the supersonic microjets with the appropriate magnitude and frequency at the desired time instants. In contrast to the traditional passive control methods, the present control-on-demand system can be switched on and off strategically. Therefore, it will not degrade the operational performance of the aircraft when it is not needed. The very small size of the actuator hardware and the minimal mass flow rates requires minimal power consumption and is expected to result in negligible thrust loss of the primary jet. In the control scheme discussed in this paper, a total of 16 supersonic microjets were distributed around the nozzle exit. A more detailed description of the microjet hardware will be provided in the experimental setup section.

II. Experimental Setup and Procedures

The experiments were carried out at the STOVL supersonic jet facility of the Fluid Mechanics Research Laboratory located at the Florida State University. A schematic of the facility with a single impinging jet is shown in Fig. 1. The measurements were conducted using an axisymmetric, convergent–divergent (C–D) nozzle with a design Mach number of 1.5. The throat and exit diameters (d and d_e) of the nozzle are 2.54 and 2.75 cm (Figs. 1 and 2). The divergent part of the nozzle is a straight-walled conic section with a 3-deg divergence angle from the throat to the nozzle exit. Although tests were conducted over a range of nozzle pressure ratios (NPR), where the NPR is equal to stagnation pressure/ambient pressure, the results discussed in the present paper are limited to NPR = 3.7 and 5. NPR = 3.7 corresponds to an ideally expanded Mach 1.5 jet, whereas NPR = 5 produces a moderately underexpanded jet. A circular plate of diameter D (25.4 cm $\sim 10d$) was mounted flush with the nozzle exit. The circular plate, henceforth referred to as the lift plate, represents a generic aircraft planform and has a central hole, equal to the nozzle exit diameter, through which the jet is issued (Fig. 2). A 1 m × 1 m × 25 mm aluminum plate serves as the ground plane and is mounted directly under the nozzle on a hydraulic lift. To visualize the flowfield in the cross plane of jet, the

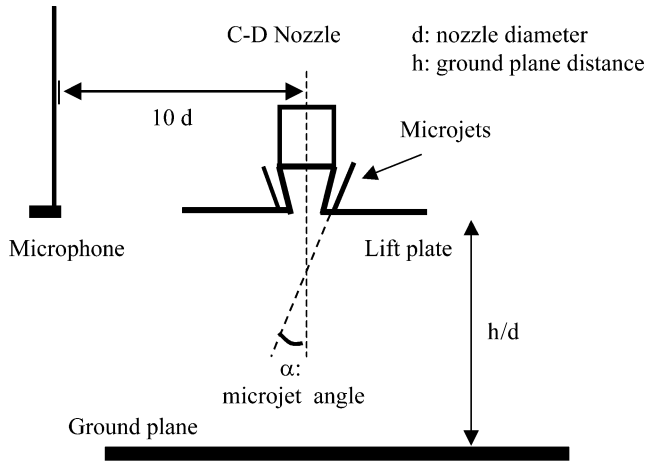

Fig. 1 Schematic of the experimental arrangement.

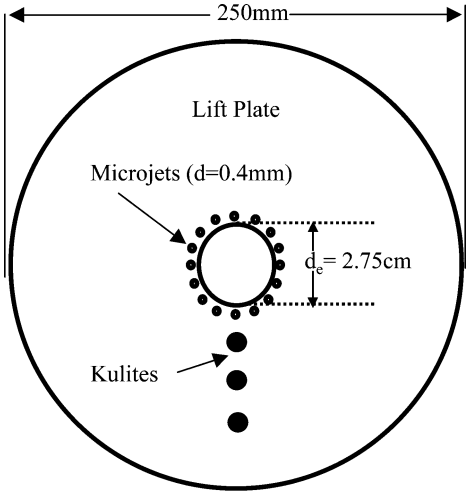

Fig. 2 Geometry of lift plate with microjets.

center part of ground plane was replaced by a glass plate for these experiments. A charge-coupled device (CCD) camera was mounted under the ground plane, beneath this window, and was used to record the jet cross plane, planar laser scattering (PLS) images presented later in this paper.

The unsteady loads generated by the impinging jet flow were measured using high-frequency response miniature Kulite® transducers on the lift plate and the ground plane. For the lift plate, three transducers (Model XCS-062) were mounted, 35, 45, and 58 mm, respectively, away from the center of nozzle. Because the signal measured by all three Kulites on the lift plate depicts similar trends, unless otherwise noted, only data from the Kulite closest to the nozzle are shown in this paper. The unsteady pressure field created by the jet impingement on ground plane was measured with three high-frequency Kulite pressure transducers (Model XCQ-062, 100 psi or 791 kPa), but only the data from the Kulite located on the jet centerline are shown in this paper. In addition, near-field noise was measured using $\frac{1}{4}$-in.-diam B&K® microphones placed approximately 25 cm away from the nozzle exit, oriented 90 deg to the jet axis (Fig. 1). To minimize sound reflections during the near-field acoustic measurements, nearby exposed metal surfaces were covered with 10-cm-thick acoustic foam.

The microphone and the unsteady pressure signals were acquired through National Instruments digital data acquisition cards using LabView® software. For unsteady measurements, that is, microphone and Kulite pressures, 100,000 points were recorded for each signal. Standard statistical analysis techniques were used to obtain the spectral content and the OASPL from these measurements. The spectral content of the unsteady signals was obtained by segmenting each data record into 100 subgroups with 1000 points each and a fast Fourier transform (FFT) with a frequency resolution of 68.4 Hz was computed for each segment. The 100 FFTs thus obtained were averaged to obtain a statistically reliable estimate of the narrowband noise spectra. The estimated uncertainty associated with the unsteady lift plate pressure P_{rms} is ±0.02 psi, whereas the rms intensities of the ground plane pressures were estimated to be accurate within ±0.2 psi. The microphone signal was measured with an estimated uncertainty of ±1 dB.

The flow was visualized using a conventional single-pass shadowgraph in a z-type arrangement. A stroboscopic white-light flash unit with a variable pulse frequency of up to 1 kHz was used as a light source. Crossflow shear layer properties were examined by the PLS visualization technique. A laser sheet, generated by a Spectra Physics Nd-YAG pulsed laser, was projected normal to the primary jet axis. Light scattered by the condensed water droplets in the mixing region renders the shear layer visible, and these PLS images were recorded by a CCD camera. These condensed droplets are formed when warm, humid ambient air comes into contact with the cold air in the jet. Note that similar flow visualization techniques have also

often been used to estimate the level of scalar mixing in the shear layer.

The main controlling parameter in the experiment was the ground plate height h with respect to the nozzle exit; this was varied from $2d$ to $60d$. The experiments were conducted over a range of NPR. The jet stagnation temperature was maintained at $20 \pm 2^{\circ}$C. The nominal exit Reynolds number at exit of the nozzle was 7×10^5 (based on exit velocity and nozzle diameter).

Active flow control was implemented using 16 microjets, flush mounted circumferentially around the main jet as shown in Fig. 2. The jets were fabricated using 400-μm-diam stainless tubes and were oriented at approximately 20 or 90 deg with respect to the main jet axis. The air supply for the microjets was provided from compressed nitrogen cylinders through a main and four secondary plenum chambers. In this manner, the supply pressures to each bank of microjets could be independently controlled. (See Alvi et al.[13] for details.) The microjets were operated over a range of NPR = 5–7, where the combined mass flow rate from all of the microjets was less than 0.5% of the primary jet mass flux.

III. Results and Discussion

A. Review of Prior Microjet Control Studies

It has been clearly demonstrated in earlier studies[13,14] that the microjets are effective in reducing both the impinging tones and the overall noise level for supersonic impinging jets. The key results from our previous work will be briefly summarized in the following paragraphs to provide the background and context for present study. Figure 3 shows representative shadowgraphs for the impinging jet flowfield at $h/d = 4$, with and without control. The presence of multiple, strong acoustic waves, marked in the instantaneous shadowgraph for the uncontrolled case, that is, microjets off, clearly signify the presence of acoustic tones. The emergence of large-scale structures in the shear layer, which are responsible for the generation of acoustic tones on impingement on the ground plane, is also evident in Fig. 3. Furthermore, the enhanced entrainment associated with such structures is also thought to be responsible for the lift loss suffered by STOVL aircraft during hover.[4,13] The instantaneous shadowgraph in Fig. 3b shows the visual effect of microjet control on this flow. The effect is visually dramatic: The large-scale structures have been significantly reduced when the microjets are on, and this is accompanied by an almost complete disappearance of the strong acoustic waves in the near field. Also visible in Fig. 3b are the streaks generated by the supersonic microjets. Note that such streaks are very similar to those generated by tabs[6] and tapes[15] and have been taken as an indicator of the presence of streamwise vorticity. Therefore, it is speculated that the production of streamwise vorticity might be responsible for the reductions in the flow unsteadiness; this is further discussed in Sec. III.C.

The visual impact of the microjets translates to a correspondingly significant effect on the unsteady pressure/noise field generated by this flow. Figure 4 shows the narrowband spectra for the unsteady pressure on the ground plane and the near-field noise for NPR 3.7, $h/d = 4$. The lift plate unsteady pressure spectrum shows an almost identical trend and is, therefore, not presented here. Upon comparing the uncontrolled data (solid lines) to the controlled case (dashed lines), one observes that the distinct tones present in the uncontrolled

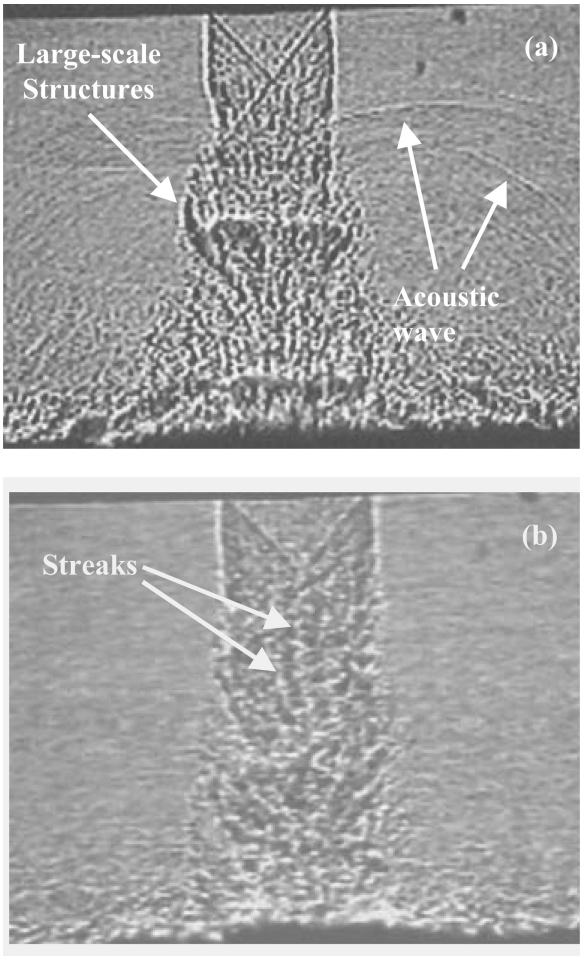

Fig. 3 Instantaneous shadowgraph images, NPR = 3.7 and $h/d = 4$: a) no control and b) with control.

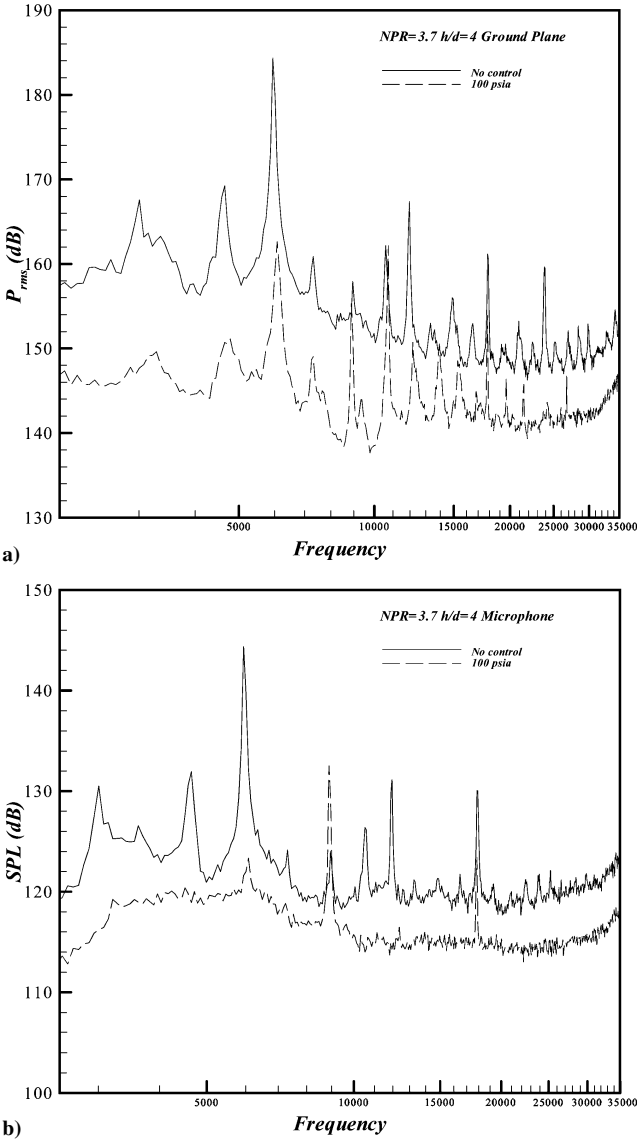

Fig. 4 Unsteady pressure and microphone spectra for NPR = 3.7 and $h/d = 4.0$: a) ground plane and b) microphone.

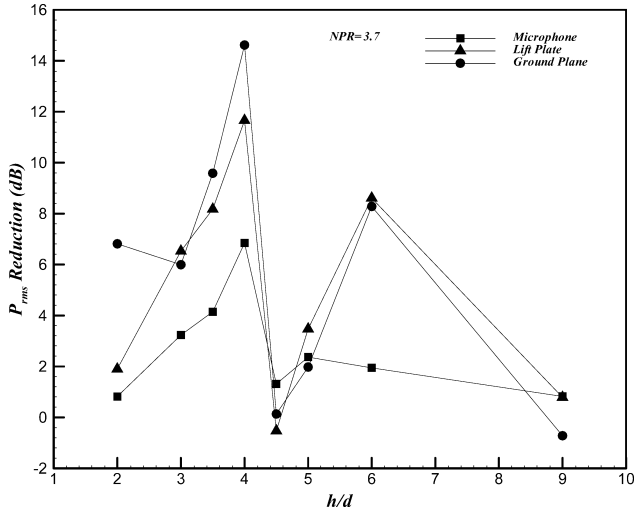

Fig. 5 Reductions in fluctuating pressure intensities as a function of *h/d*, NPR = 3.7, 20-deg microjets.

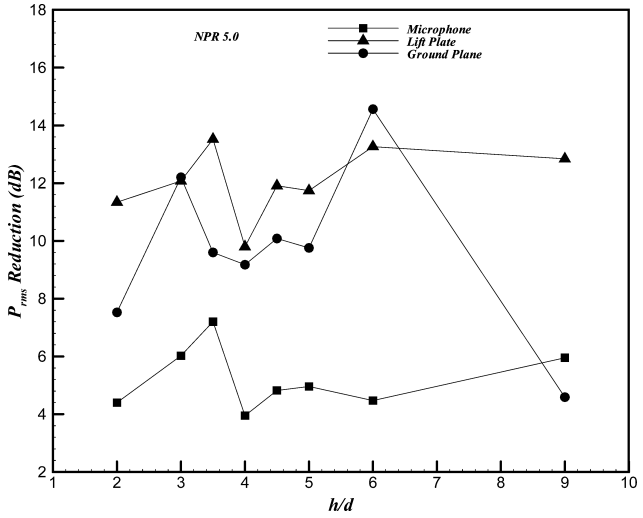

Fig. 6 Reductions in fluctuating pressure intensities as a function of *h/d*, NPR = 5 and 20 deg microjets.

impinging jet are either entirely eliminated or significantly diminished by the activation of microjets. In addition, and perhaps more significantly, the attenuation in the discrete tones is accompanied by a broadband reduction in the spectral amplitudes. This broadband reduction is observed for all spectra due to lower acoustic and pressure fluctuations, which indicates an overall decline in the unsteadiness of the flow when control is implemented.

The overall reduction in the unsteady pressure levels P_{rms} on the lift plate, the ground plane, and in the near-field noise is shown in Figs. 5 and 6 for NPR = 3.7 and 5, respectively. Although a range of microjet pressures were tested, the data shown in Figs. 5 and 6 correspond to the microjets operating at ~100 psia. (The effect of microjet pressure on control efficiency will be discussed later.) The trends observed here are very similar to those obtained at other microjet pressures. Figures 5 and 6 clearly show that the fluctuating loads are significantly reduced at all three measurement locations for both NPR, at almost all heights. However, the magnitude of reduction is strongly dependent on the ground plane distance (h/d) and to a lesser degree on the NPR.

In general, the microjets are more effective for the underexpanded jet (NPR = 5), where the lift and ground plate pressures are reduced by 10–14 dB and the near-field noise by 5–6 dB. However, for a given NPR, the magnitude of reduction is strongly dependent on the ground plane distance (h/d). The variation of the level of reduction appears to have a staging behavior, as seen in Fig. 5. This trend of nonuniform reductions for the microjet control might be related to the well-known staging behavior of the impingement tones with ground plane distance, as discussed in some detail by Krothapalli et al.[4] The nonuniform reductions indicate that the control technique is not equally efficient at all heights presumably because it does not track changes in the feedback loop due to variations in h/d. This suggests that efficient control of this flow requires an adaptive control approach where the microjet operating parameters need to be adaptively manipulated to provide optimal control at all heights.

B. Present Results: Effect of Microjet Operating Parameters and Configurations

A comprehensive parametric study, examining the effect of microjet control parameters and configurations on the overall flow control efficacy has been conducted to find the means for devising optimum control strategies. These experiments, which cover a large parametric space, also provide some insight on the physical mechanisms behind the present microjet control technique. With this in mind, the parameters varied include the microjet operating pressure, the microjet angle, the use of microtabs instead of microjets, the microjet size, the number/spacing of microjets, and the spatial distribution of microjets relative to the main jet. For the sake of brevity, the effect of varying the first three parameters is discussed in this paper because they appear to play a primary role in determining control efficiency.

1. Microjet Angle

The first parameter examined is the microjet angle with respect to the main jet flow. The microjet operating pressure is fixed at 100 psi for the results discussed in this subsection. For the lift plate, the data from a Kulite mounted at a distance of about 45 mm from the center of the nozzle is compared here. It has been shown that the 20-deg microjet is more effective for underexpanded conditions relative to ideally and overexpanded cases. It was first thought that this difference was due to the concave curvature of the jet boundary when the jet is operated at underexpanded conditions. The emergence of a concave jet shear layer at the nozzle exit makes it easier for the microjet streams to perturb the primary shear layer. As a secondary effect, we anticipated that the microjets placed at a smaller angle could partially shield the local shear layer from the upstream acoustic waves more effectively than higher microjet angle case, thus further weakening the feedback loop.

For the ideally expanded case shown in Fig. 7, the unsteady pressure reductions due to microjet control increase for almost all heights when the angle is changed from 20 to 90 deg. For the sake of brevity, only data from transducer on the lift plate are shown in Fig. 7; however, the trends discussed here are observed for all measurement locations, that is, in the microphone and ground plane measurements.

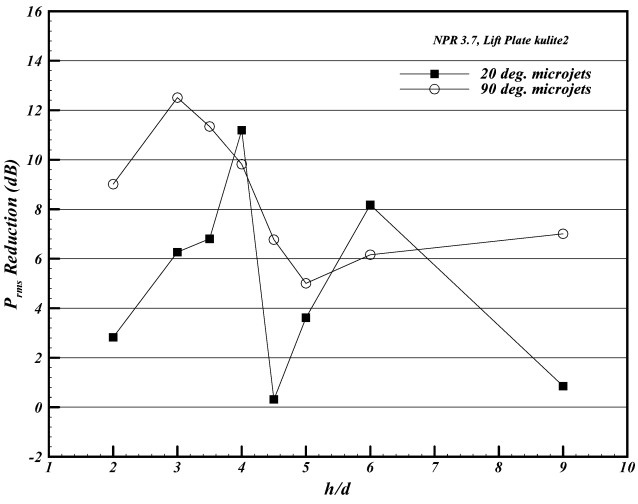

Fig. 7 Reductions of fluctuating pressure intensities, NPR = 3.7, 20-deg vs 90-deg microjet control, lift plate.

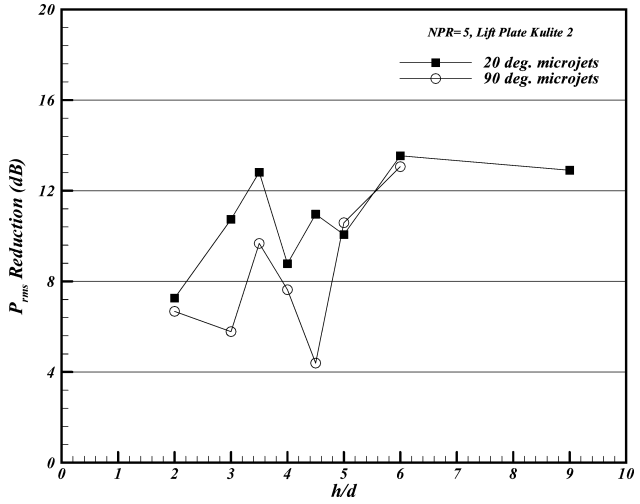

Fig. 8 Reductions of fluctuating pressure intensities, NPR = 5.0, 20-deg vs 90-deg microjet control, lift plate.

This increase in the control efficacy is quite substantial in that the unsteady pressure loads are attenuated by an additional 5–8 dB relative to the 20-deg microjets. The change is even more dramatic at certain heights, such as $h/d = 2$, 4.5, and 9, which show minimal reduction with the 20-deg microjets. In contrast, the use of 90-deg microjets reduced the aeroacoustic loads by at least 7 dB at these heights. Recalling that the 90-deg microjets do not intercept the acoustic waves, but still manage to provide more effective control than 20-deg microjet, clearly indicates that the shielding from, or the interception of, the acoustic waves by the microjet streams is not the primary mechanism behind this control scheme.

In contrast, the trends observed in Fig. 8 are the opposite of those seen in Fig. 7. For the underexpanded case shown in Fig. 8, the attenuations due to the 90-deg microjets are somewhat smaller at almost all of the heights when compared to the noise reduction efficacy for the 20-deg microjets. However, a careful examination of the OASPL data without control for NPR = 5 indicates that this apparent difference in control efficiency is primarily due to the difference in the unsteady pressure levels for the baseline (uncontrolled) cases, that is, between the 90- and 20-deg configurations. To illustrate this, in Fig. 9a we compare the P_{rms} at the ideally expanded condition, NPR = 3.7. As expected, the values are almost identical for the baseline/no-control condition. In contrast, for the underexpanded condition, as seen in Fig. 9b, a comparison of the P_{rms} levels between 20-deg microjet (open squares) and 90-deg microjet (open circles) reveals that the baseline P_{rms} is significantly lower with the 90-deg microjet configuration. Because the P_{rms} values with control are very similar for the 20-deg microjets (filled squares) and 90-deg microjets (filled circles) as seen in Fig. 9b, the net reduction with the 90-deg microjets is lower due to lower baseline values (open circles).

The reason behind this apparent discrepancy in the baseline P_{rms} values can be explained by examining the microjet configuration on the lift plate. When placed at a 90-deg angle, the microjet nozzle exit is essentially perfectly aligned with the edge of the primary nozzle. As such, the microjet nozzles should have a minimal, if any, effect on the primary jet flowfield at the ideally expanded condition because the jet boundary does not interact with the microjets when the microjets are off. Consequently, the baseline values for the 20- and 90-deg microjets are essentially the same (open symbols, Fig. 9a). However, at the underexpanded condition, the bulging of the jet column due to the expansion waves at the nozzle causes the shear layer of the primary jet to interact with the 90-deg microjet nozzles and these micronozzles now extend into the jet shear layer even when the microjet are off. As a matter of fact, one can consider these microjet tubes as miniature tabs protruding inward from the primary jet nozzle. Consequently, the presence of 90-deg micronozzle itself results in streamwise vorticity in an underexpanded jet even without activating the microjet control. This line of reasoning is supported

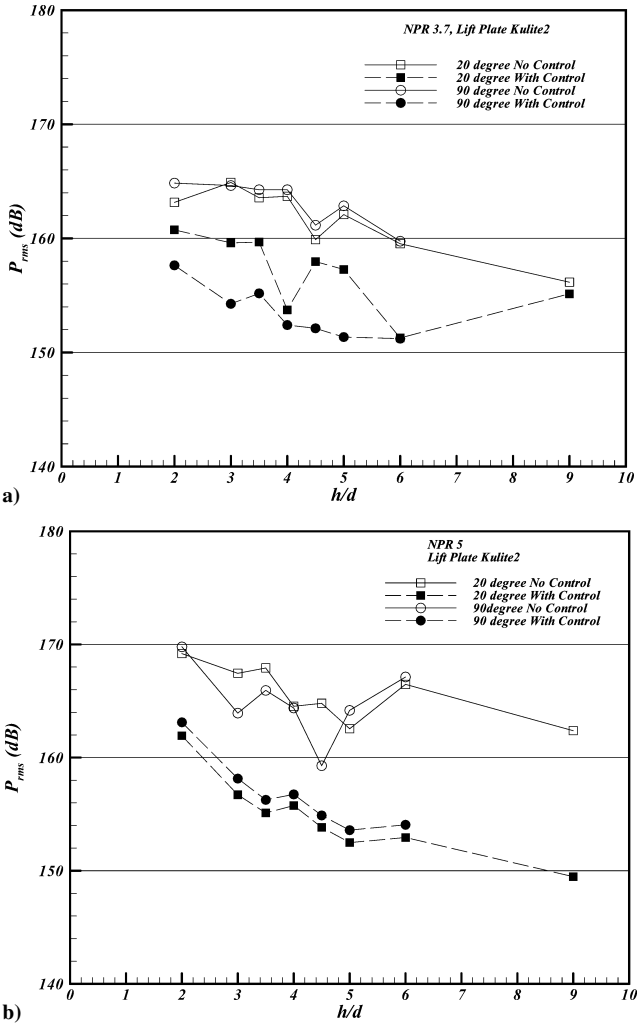

Fig. 9 Unsteady pressure intensities, lift plate: a) NPR = 3.7 and b) NPR = 5.

by our experiments when the microjets are replaced by microtabs, discussed in Sec. III.B.3.

2. Microjet Pressure

Another factor that is expected to contribute to the efficiency of microjet control is the "penetration depth" of the microjet stream into the primary jet shear layer. It has been shown[16] that a stronger microjet stream with a longer supersonic core length can be generated if the microjets are operated at a higher stagnation pressure. Consequently, the effect of microjet pressure on control efficiency was examined. The effects of this parameter in reducing the flow unsteadiness are shown in Figs. 10 and 11 for NPR 3.7 and 5, respectively, using the 20-deg microjets.

For the results shown here, the microjet pressure is increased from 80 to 120 psia in increments of 10 psi. For the ideally expanded case shown in Fig. 10, the attenuation in P_{rms} increases relatively fast as the microjet pressure is increased from 80 to 100 psia. Beyond this value, the gains in performance, that is, P_{rms} reductions, become increasingly small at most heights. For the present study, the performance of the 20-deg microjets is near saturation at approximately 100 psi. Hence, in terms of performance vs cost, cost being the microjet pressure, increasing the pressure beyond 100 psi yields very little dividends. This is the reason that for most of the cases discussed in this paper the microjets are operated at 100 psi.

The results are somewhat different when the primary jet is operating at an underexpanded condition, as shown in Fig. 11. As seen from Fig. 11, increasing the microjet pressure from 80 to 120 psi has a negligible effect on performance. This is because saturation in performance occurs at pressures below 80 psi, roughly around

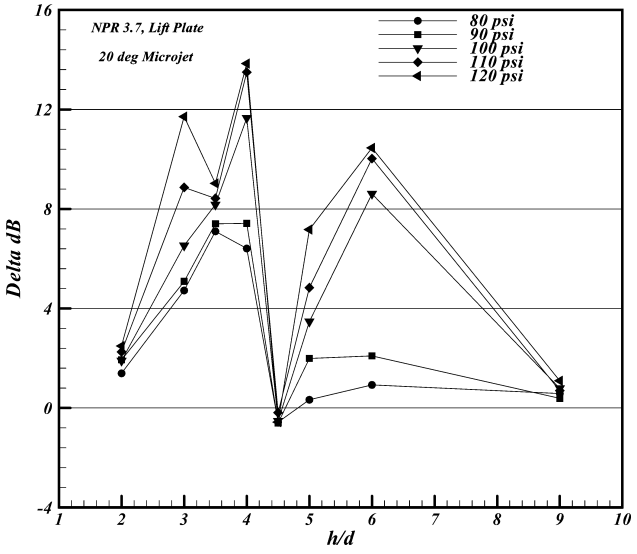

Fig. 10 Reductions of fluctuating pressure intensities on lift plate for different microjet pressures: NPR = 3.7, 80–120 psia.

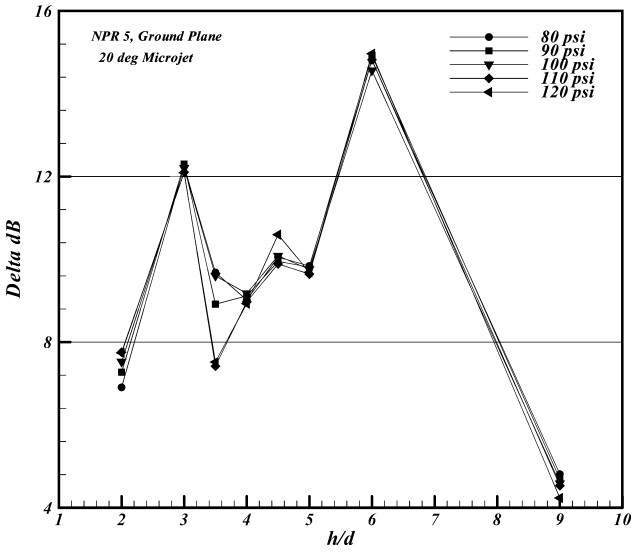

Fig. 11 Reductions of fluctuating pressure intensities on ground plane for different microjet pressures: NPR = 5, 80–120 psia.

50–60 psi, for the underexpanded case. These results indicate that increasing the pressure significantly above saturation levels does not change the system behavior or lead to any further performance gains. As already mentioned, in general, the overall reductions in the pressure fluctuations are much better for the underexpanded jet at nearly all h/d (order of 10–14 dB) relative to that for the ideally expanded jet (Fig. 10).

It is expected that the effective penetration depth is longer for the underexpanded case because the jet boundary expands outward to compensate for the difference between the higher pressure at the nozzle exit and the ambient pressure. On the other hand, the jet boundary expansion is more moderate for the ideally expanded case and actually experiences a contraction for the overexpanded condition. Shorter penetration depth means less influence on the jet flowfield for over and ideally expanded cases. The opposite is true for the underexpanded case.

3. Microtabs

As discussed in the Introduction, tabs have been used in many studies, relatively recently by Samimy et al.,[6] for controlling the aeroacoustic behavior of freejets. Samimy et al.[6] found their tabs to be effective in reducing screech noise for underexpanded jets where

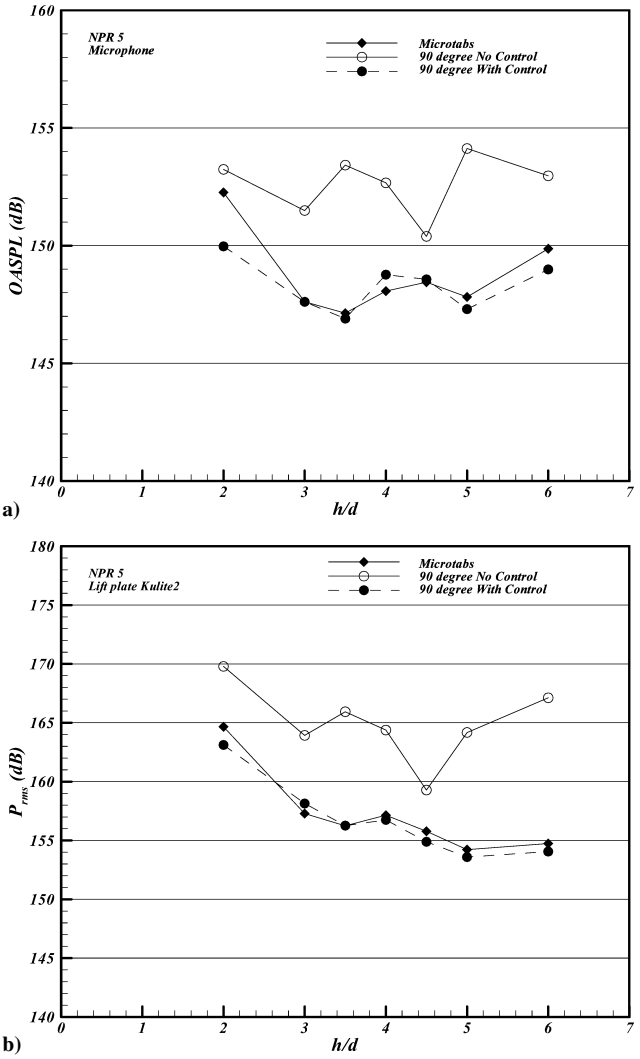

Fig. 12 Reductions of fluctuating pressure intensities for microtabs vs 90-deg microjets and no control data, NPR = 5: a) microphone and b) lift plate.

they were also shown to enhance mixing in the jet shear layer. Using the flow visualization results (PLS images), Samimy et al.[6] argued that their tabs produce significant streamwise vorticity through pairs of "trailing vortices" and it is this vorticity that is primarily responsible for altering the jet aeroacoustic properties. Motivated by their results and those of similar tab studies, we examined the use of tabs for impinging jet flows, hoping that these results would also provide further insight into the flow physics behind microjet control.

In the present study, microtabs are made by inserting a thin stainless wire (400 μm diameter) into the 90-deg microjet nozzles. The stainless steel microtab extends 2.5 mm (approximately 10% of the primary jet diameter) into the main jet. Figures 12 and 13 show the comparison between the microtabs and the 90-deg microjets for NPR = 5 and 3.7, respectively, where the microjets are operated at 100 psi. For the underexpanded case shown in Fig. 12, microtab control produces an effect almost identical to the microjets. This suggests that, at least for the underexpanded jet, the control mechanism behind microtabs and microjets is very similar. That is, they both reduce flow unsteadiness, perhaps by the production of streamwise vorticity through the counter-rotating streamwise vortex pairs generated by the microtabs, in a manner similar to that suggested by Samimy et al.[6]

In contrast, the effect of microtabs on controlling the ideally expanded impinging jet, shown in Fig. 13, is considerably less impressive than the 90-deg microjets. Whereas microjet control yields P_{rms} reductions as high as 15 dB (Fig. 13b), the microtabs reduce

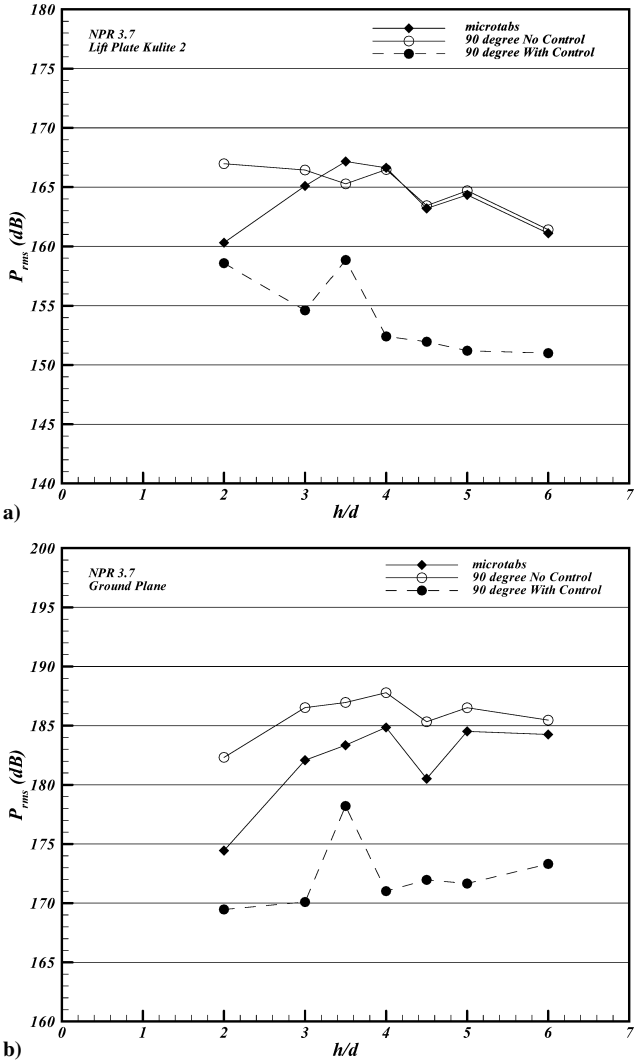

Fig. 13 Reductions of fluctuating pressure intensities for microtabs vs 90-deg microjets and no control data, NPR = 3.7: a) lift plate and b) ground plane.

the unsteady loads between 2 and 5 dB at corresponding locations. In fact, the microtabs have almost no impact on the near-field noise attenuation, as seen in Fig. 13a. We note that our results do not preclude the fact that if larger tabs were used, such as those used in previous studies, they would be effective. However, larger tabs have higher losses associated with them and are, thus, less practical. Furthermore, in the present study, our aim is to compare our active fluidic-based control approach with a passive method where both actuators are of comparable size.

As such, our results suggest that if vorticity generation is indeed the main physical phenomenon behind microjet and microtab control then the mechanisms by which it is generated and/or redistributed are different for the two actuators. A better understanding of the underlying mechanisms behind microjet control is necessary for the development of an effective scheme; this is discussed next.

C. Possible Physical Mechanisms

A brief discussion of some of the physical mechanisms that are expected to play a role in the present and previous control studies was presented in the Introduction; a more comprehensive discussion in the context of the present, microjet-based control, approach is presented here. It was initially anticipated that the supersonic microstreams may intercept the upstream propagating acoustic waves. This would, at least partially, weaken the interaction between the acoustic waves and jet shear layer at the nozzle lip, hence, attenuating the feedback loop. Based on the fact that the 90-deg microjets placed at the nozzle exit cannot intercept the acoustic waves, but still provide very effective control, better than the 20-deg microjets for most cases, it appears that this acoustic shielding is not a fundamental mechanism behind the present control approach. Although the blocking of the acoustic waves does work when the shielding device is sufficiently large, as illustrated in the experiments of Elavarasan et al.,[9] it is not significant in the present control scheme, presumably because of the very small size of the microjets.

The results presented earlier clearly demonstrate that microjet control is more effective for underexpanded condition relative to both ideally and overexpanded conditions. (For example, compare Figs. 5 and 6.) This observation is consistent with our earlier assertion that the streamwise vorticity, whose presence is suggested by the streaks seen in the shadowgraphs (Fig. 3b), might be responsible for the attenuation of the feedback loop. It is well known that the streamwise vorticity generation and growth is enhanced in the presence of a highly concave shear layer, such as the curved shear layer on the jet periphery when a jet is operating at an underexpanded condition. Therefore, if the generation of streamwise vorticity is a principal mechanism behind the present microjet control, it is expected that perturbing an underexpanded jet is much easier than an ideally expanded or an overexpanded jet. Experiments for the underexpanded cases show that the use of microtabs produces the same control effect as the microjets (Fig. 13), further support our hypothesis regarding the role of streamwise vorticity.

To further examine the streamwise flow structures produced by the activation of the microjets, a PLS technique was used where a laser sheet was oriented perpendicular to the main jet axis, thus providing cross-stream images of the jet. Instantaneous and time-averaged images for an underexpanded jet (NPR = 5), with and without control, are shown in Figs. 14 and 15. These images were taken one diameter downstream of the jet. Without microjet control, weak indentations can be observed around the condensation ring, seen in the instantaneous PLS image in Fig. 14a. As noted by Krothapalli et al.,[15] among others, these indentations are generally considered to be indicative of the presence of counter-rotating vortex pairs. Much more clearly defined indentations emerge when the microjets are turned on, and one can identify a total of 16 of these modulations in the microjet-controlled jet shear layer seen in Fig. 14b. Time-averaged images (where each image is an ensemble average of over 20 instantaneous snapshots) such as those shown in Fig. 15, reveal the presence of these vortex-induced indentations more clearly. Without control, the shear layer appears as a smooth ring structure in Fig. 15a, indicating that some of the structures seen in the uncontrolled jet (Fig. 14a) are not spatially stationary. In contrast, with microjet control, the averaged pattern displays a strongly modulated ring with a total of 16 indentations. Moreover, these indentations align with the azimuthal location of the microjets placed at the periphery of the primary jet nozzle. The vortex structures become more diffused as one proceeds farther downstream with fewer indentations visible at two jet diameters (not shown here). This suggests a merging and diffusion of the streamwise vortices, a behavior observed by other investigators.

Having presented evidence of the occurrence of significant streamwise vorticity when the microjets are activated, one must then ask what is the source of these streamwise vortices? In the study where tabs were used to control jet aeroacoustics, Samimy et al.[6] proposed that these vortices are a result of the substantial pressure differential that exists between the upstream and downstream sides of the tabs. These strong streamwise vortices modulate the primary vortical structures in the main jet shear layer, which in turn reduces the azimuthal coherence of the primary vortices and make them less sensitive to the upstream-propagating acoustic excitations.

However, the different control effect of microjets and microtabs for an ideally expanded jet suggests that the streamwise vorticity using microjets may be generated and evolve through different mechanisms. In the microjet control case, one potential source of the streamwise vorticity is the vorticity contained in the microjet streams. Based on simple dimensional analysis, one can easily show that the collective circulation from all microjets is minimal

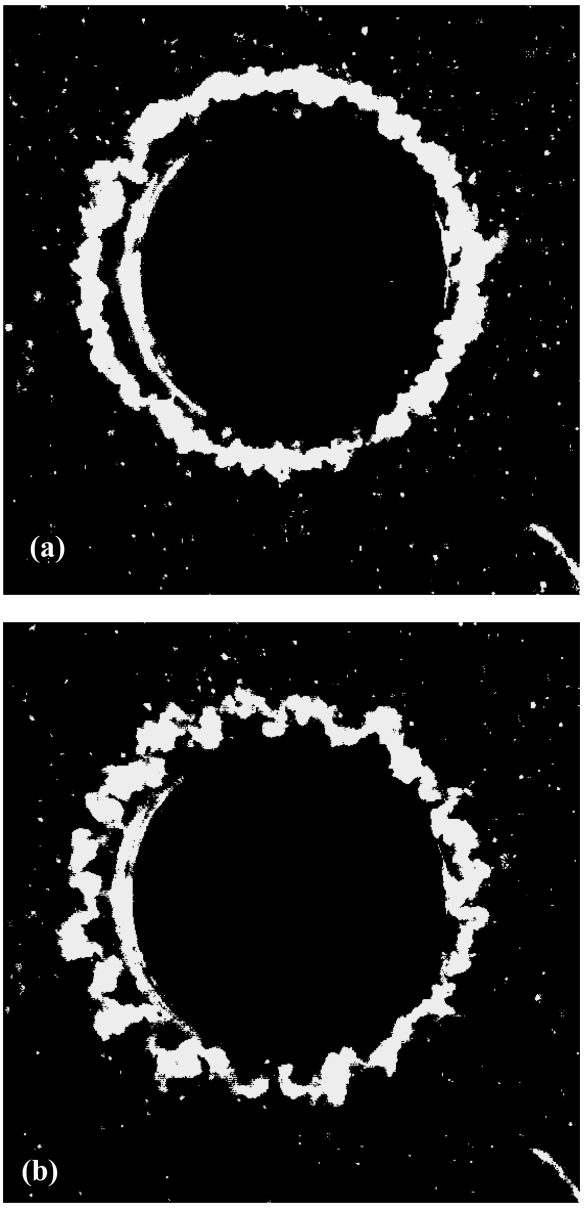

Fig. 14 Instantaneous PLS images taken one diameter downstream of the nozzle, NPR = 5, $h/d = 4$: a) no control and b) with control.

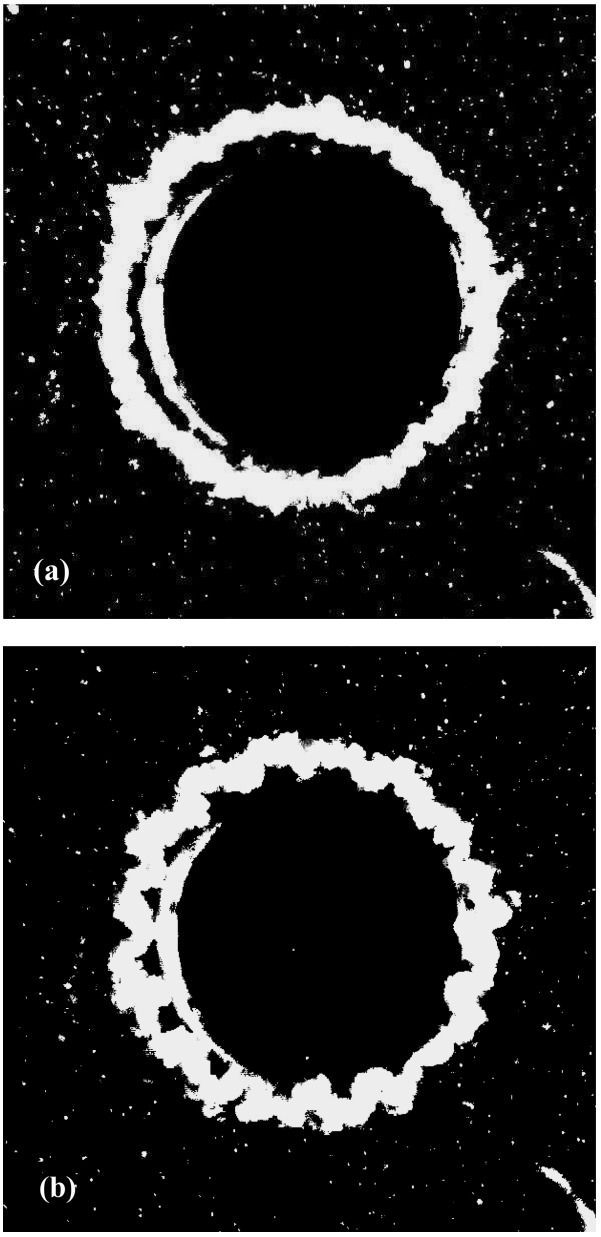

Fig. 15 Time-averaged PLS images taken one diameter downstream of the nozzle, NPR = 5, $h/d = 4$: a) no control and b) with control.

as compared to the circulation of the primary jet. Thus, it is not possible for the vorticity in the microjets to be the sole source of these strong streamwise vortices. Therefore, the streamwise vorticity must come from the primary jet vorticity. It is speculated that microjet control redirects the primary vorticity into streamwise direction through two primary processes: vorticity tilting and vorticity stretching.

Vorticity tilting is the reorientation of the vortex element as the result of a locally nonuniform velocity distribution. In the current situation, the microjet stream can redirect the significant azimuthal vorticity component present in the uncontrolled jet (seen as large-scale structures in the uncontrolled jet in Fig. 3a) into either the transverse or streamwise direction, thus reducing the primary shear layer vorticity and weakening the azimuthal structures.

Once the vortex element is tilted by the microjet in the streamwise direction, it experiences a stretching or compression depending on main jet flow condition. In the underexpanded jet, the streamwise vorticity is stretched due the local flow acceleration. As a result, this stretching can strengthen the displaced vortex element and generate enough perturbations in the shear layer so that the azimuthal coherence of the coupling between the acoustic waves and flow instabilities cannot be effectively established. However, in an overexpanded jet, the displaced vortex is suppressed due to flow deceleration. This is consistent with the fact that microjet control is most effective for an underexpanded jet and not as effective for an ideally and overexpanded jet. It is believed that these vorticity titling and stretching mechanisms are important elements responsible for the current microjet control. The end result of this vorticity generation and redirection is a significant reduction of the feedback loop coupling and an overall reduction of the flow instability.

IV. Summary

In this paper, a systematic study of control parameters governing microjet control was carried out. Parameters studied include microjet angle, microjet pressure, and the use of microtabs. For an ideally expanded jet, a marked improvement in the reduction of the flow unsteadiness can be achieved if the microjet angle is changed from 20 to 90 deg, whereas this angle change has little or no effect for the underexpanded jet. The effectiveness of microjet control depends strongly on the microjet pressure for an ideally expanded jet but is less sensitive when jet is operating at underexpanded conditions.

This is because saturation is reached at relatively low microjet pressures. Microtabs produce the same control effect as 90-deg microjets for an underexpanded jet, yet they have a negligible effect on an ideally expanded mode.

The role of streamwise vorticity, generated by the microjets and enhanced (or suppressed) through the vorticity tilting and stretching mechanisms, is discussed phenomenologically. It is suggested that this may be a principal physical mechanism behind the success of the present control technique, which has proven to be very effective in reducing flow unsteadiness. Based on a better understanding through these results, it is anticipated that a microjet-based control strategy that produces a more uniform control effect for all configurations can be developed.

Acknowledgments

This work was supported by a grant from the Air Force Office of Scientific Research monitored by J. Schmisseur. We are grateful for this support. We thank the staff of the Fluid Mechanics Research Laboratory for their invaluable help in conducting these tests. We are grateful for the assistance provided by B. Alkislar in making the particle image velocimetry measurements and I. Choutapalli for his help in conducting the tests.

References

[1]Powell, A., "The Sound-Producing Oscillations of Round Underexpanded Jets Impinging on Normal Plates," *Journal of the Acoustical Society of America*, Vol. 83, No. 2, 1988, pp. 515–533.

[2]Neuwerth, G., "Acoustic Feedback of a Subsonic and Supersonic Free Jet Which Impinges on an Obstacle," NASA TT F-15719, May 1974.

[3]Tam, C. K. W., and Ahuja, K. K., "Theoretical Model of Discrete Tone Generation by Impinging Jets," *Journal of Fluid Mechanics*, Vol. 214, May 1990, pp. 67–87.

[4]Krothapalli, A., Rajakuperan, E., Alvi, F. S., and Lourenco, L., "Flow field and Noise Characteristics of a Supersonic Impinging Jet," *Journal of Fluid Mechanics*, Vol. 392, Aug. 1999, pp. 155–181.

[5]Powell, A., "The Reduction of Chocked Jet Noise," *Proceedings of Physics Society B*, Vol. 67, No. 4, 1954, pp. 313–327.

[6]Samimy, M., Zaman, K. B. M. Q., and Reeder, M. F., "Effect of Tabs on the Flow and Noise Field of an Axisymmetric Jets," *AIAA Journal*, Vol. 31, No. 4, 1993, pp. 609–619.

[7]Kim, J. H., and Samimy, M., "Mixing Enhancement via Nozzle Trailing Edge Modifications in a High Speed Rectangular Jet," *Physics of Fluids*, Vol. 11, No. 9, 1999, pp. 2731–2742.

[8]Karamcheti, K., Bauer, A. B., Shields, W. L., Stegen, G. R., and Woolley, J. P., "Some Features of an Edge Tone Flow Field," NASA SP 207, 1969, pp. 275–304.

[9]Elavarasan, R., Krothapalli, A., Venkatakrishnan, L., and Lourenco, L., "A PIV Study of a Supersonic Impinging Jet," *Journal of Visualization*, Vol. 2, No. 3/4, 2000, pp. 213–222.

[10]Sheplak, M., and Spina, E. F., "Control of High-Speed Impinging-Jet Resonance," *AIAA Journal*, Vol. 32, No. 8, 1994, pp. 1583–1588.

[11]Shih, C., Alvi, F. S., and Washington, D., "Effects of Counterflow on the Aeroacoustic Properties of a Supersonic Jet," *Journal of Aircraft*, Vol. 36, No. 2, 1999, pp. 451–457.

[12]Alvi, F. S., and Iyer, K. G., "Mean and Unsteady Flowfield Properties of Supersonic Impinging Jets with Lift Plates," AIAA Paper 99-1829, May 1999.

[13]Alvi, F. S., Shih, C., Elavarasan, R., Garg, G., and Krothapalli, K., "Control of Supersonic Impinging Jet Flows Using Supersonic Microjets," *AIAA Journal*, Vol. 41, No. 7, 2003, pp. 1347–1355.

[14]Shih, C., Alvi, F. S., Lou, H., Garg, G., and Krothapalli, A., "Adaptive Flow Control of Supersonic Impinging Jets," AIAA Paper 2001-3027, June 2001.

[15]Krothapalli, A., Strykowski, P. J., and King, C. J., "Origin of Streamwise Vortices in Supersonic Jets," *AIAA Journal*, Vol. 36, No. 5, 1998, 2001, pp. 869–872.

[16]Phalnikar, K. A., Alvi, F. S., and Shih, C., "Behavior of Free and Impinging Supersonic Microjets," AIAA Paper 2001-3047, June 2001.

G. Candler
Associate Editor